International Society of Experimental Hematology（2011年8月25日28日 Westin Bavshore Hotel, Vancouber, Canada）

4. 北村俊雄 Two types of C/EBPa mutations collaborate in inducing leukemia in a mouse BMT model. 第25回 IACRLRD （2011年9月15-17日 東京大学本郷キャンパス）

5. 北村俊雄 Molecular basis of leukemia,MPN and MDS 第70回日本癌学会学術総会（2011年10月3-5日名古屋国際会議場）

6. 中原史雄、北村俊雄 Molecular mechanisms of blast crisis in chronic myelogenous leukemia 第70回 日本癌学会学術総会（2011年10月3-5日名古屋国際会議場）

7. 北村俊雄 Mouse models for MDS/overt leukemia and CML-BC 第73回 日本血液学会学術集会（2011年10月14-16日 名古屋国際会議場）

8. 伊沢久未、北浦次郎、山西吉典、沖俊彦、奥村康、北村俊雄 LMIR3 ノックアウトマウスにおけるアレルギー反応の亢進 日本免疫学会（2011年11月29日 幕張メッセ）

E. 知的財産権の出願・登録状況

なし

厚生労働科学研究費補助金（第３次対がん総合戦略研究事業）
分担研究報告書

多種がんの高集積アレイを用いた分子標的抗体薬候補の特異性検討、および全身がんにおける横断的分布の観察と機能の評価に関する研究

分担研究者　富山大学附属病院外科病理学講座　福岡順也

研究要旨

抗体薬の開発は、がん細胞で活性化しているシグナル伝達系を抑制、もしくは正常化するものへと絞られてきている。また標的とする分子は、治療対象としている疾患に充分な発現を示さないと効果を期待できない事が明瞭となっており、分子の局在を観察することは極めて重要である。また、標的分子が対象疾患でどのような機能を有しているか知ることも治療の観点から重要である。結局のところ、患者の組織判定はホルマリン固定パラフィンブロックにて行われることになるので、網羅的解析をホルマリン固定後のパラフィン包埋ブロックを用いた組織アレイで検討する事は重要である。ただし、作製抗体が、うまくパラフィンブロックにて特異的な染色性を示す頻度は低い。今回、ホルマリン固定された標的分子を発現する細胞株上のエピトープを認識する複数のクローンが組織上で染色されるか検討し、それらから作製された精製抗体を用い、作製した多種癌組織アレイへの染色を行い、臨床病理学的検討を行った。その結果、抗 EphA2 抗体が大腸癌と肺がんの予後因子であることが判明した。

A.　研究目的

がんの治療は大きく分子標的薬へとシフトしており、新薬の開発は、がん細胞で活性化しているシグナル伝達系を抑制、もしくは正常化する小分子か、抗体薬へと絞られてきている。分子の検討を行う為には、標的とする分子がどの程度、治療対象としている疾患に発現しており、その局在がどこに存在するかを観察することは極めて重要である。また、標的分子の発現が対象疾患でどのような生物学的機能を有しているかの検討も治療デザインの観点から極めて重要である。しかし、このような網羅的解析を組織上にて行う事の出来るツールである組織アレイは、ホルマリン固定後のパラフィン包埋ブロックを用いて作製されるため、作製抗体が、うまく特異的な染色性を示すことの出来る頻度は低い。また、今までの分子標的薬の治療成績を見てみると、治療効果は明瞭なバイオマーカーの発現によって規定されており、同時に投薬の指標となる組織上の染色性検討を行い、診断薬と治療薬を同時に開発することが重要であることは明瞭である。患者群の選定を検討することが必須である。今回、ホルマリン固定された標的分子を発現する細胞株上の

エピトープを認識する複数のクローンのうち、組織上で染色される事を確認したものの精製抗体について脳腫瘍組織アレイと多種癌組織アレイを用い、臨床病理学的検討を行った。

B： 研究方法

＜高集積組織アレイにおける染色と評価＞
染色条件検討にて充分に特異性と感受性を有すると判断したものにおいて、精製抗体を作製し、さらに染色プロトコルを最適化したのちに高集積アレイへの染色を行った。染色スライドは全てバーチャルスライドにてスキャンを行い、ビューワー上にてスコアリングを行った。評価は細胞の局在毎、つまり細胞質、細胞膜、核ごとに評価した。それぞれの局在部位毎に強度と分布（染色範囲）を検討し、それぞれ、強度スコア：0:染色性なし、1:弱陽性、2:中等度、3:強陽性、分布スコア：0:染色性無し 1:50%未満の腫瘍細胞が陽性、2:50%以上の腫瘍細胞が陽性　と評価した。強度スコアと分布スコアの総和が 3 以上を基本的に陽性とみなした。
＜統計解析＞
染色性と組織型、分化度、性別、年齢、Stage、脈管侵襲（癌腫）の相関をχ自乗検定およびフィッシャー検定を用いて評価した。生命予後情報のある癌腫では、ログランクテストを用いて生存解析を行い、カプランマイヤー曲線をプロットした。P 値＜0.05 未満を統計学的に優位と認識した。

＜倫理的配慮＞
個人情報は非連結可能匿名化を行っている。本研究のプロトコルは富山大学倫理委員会の承認を受けている。（認１９－１２）

C： 研究成果

SST-REX 法にホルマリン固定を加えた変法にて研究代表者の北村らが作製した抗体のうち、EphA2 に対する抗体 (ACT00140-0065, clone 1CBE6-3)、Clorf56 に対する抗体 (ACT230-15, clone 2A1), FSZTL1 に対する抗体 (ACT41-385, clone 9C8H7)の 3 クローンにおいて、染色を確認し、スコアを取得、結果につき臨床病理学的検討を行った。

＜EphA2 の免疫染色＞
2 つの Clone にて組織アレイを染色した。
1）clone 1CBE6-3
細胞質＞核＞＞細胞膜に発現を認めた。特に甲状腺癌、子宮癌において高い発現が確認された。脳腫瘍では、核の染色が優位であった。

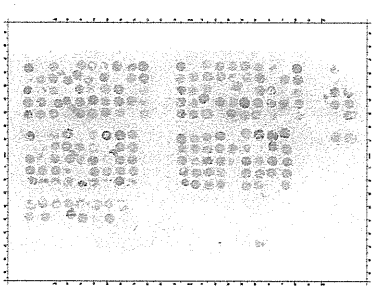

図１．脳腫瘍における発現

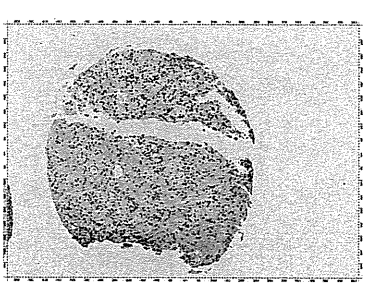

図２．核に発現が確認された。

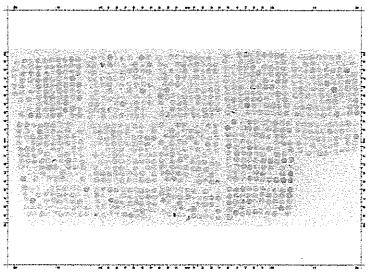

図３．組織アレイによる発現の検討

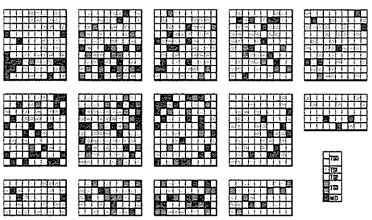

図４．組織アレイ上の染色結果マップ

発現は細胞質が中心で、核、膜にも発現が観察された。

腎癌、膀胱癌、卵巣癌において高く観察された。

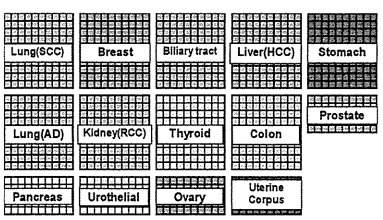

図５.多種癌組織アレイのマップ

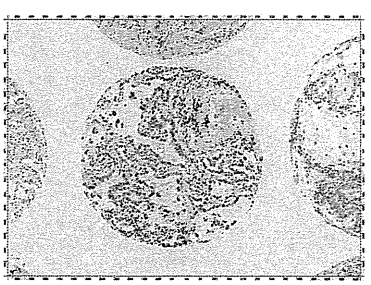

図６.肺腺癌における核主体の染色。

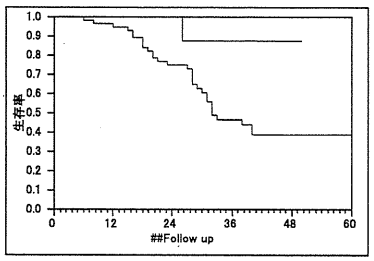

図７．肺腺癌の予後カーブ（核：青＝陽性）

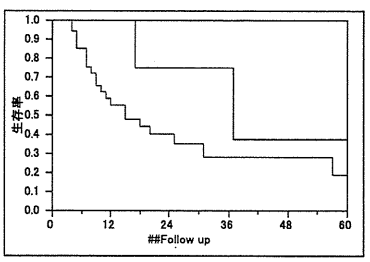

図8. 膵癌の予後カーブ(核：青＝陽性)

核の発現はやや予後良好の傾向を示し、肺腺癌では、有意差をもって予後良好因子として認識される(P=0.049)。他の癌腫では明瞭な予後の差は見られない。膵癌では、予後良好の傾向を示すものの、統計学的な有意差は見られなかった。細胞膜での発現はごくわずかであり、予後的意義は見られなかった。脳腫瘍では、明瞭な予後との相関を認めなかった。

他に肺腺がんでは、分化度との負の相関をしめし(P=0.031), 腎癌では stage との負の相関を認めた(P=0.006)。大腸癌では stage との負の相関がみられ(P=0.007)、また、少数ではあるものの、膀胱がんでは、細胞膜の発現が stage との負の相関を示した(P=0.006)。細胞質の発現では、胃がんにおいて stage との負の相関がみられた(P=0.009)。

2） Clone 6B10

Clone 6B10 も核優位の発現をしめした。よ

りubiquitousな発現を認め、大腸癌、乳癌、肺腺癌、甲状腺癌、胃癌においてより高い発現を観察した。

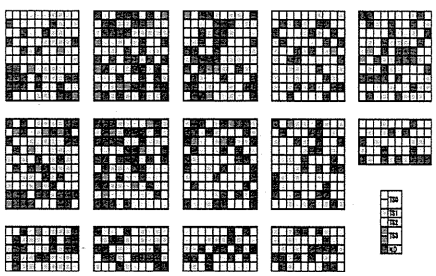

図9 Clorf56の細胞質発現

発現はclone 1CBE6-3と同様、腎癌、卵巣癌において高い傾向を示した。

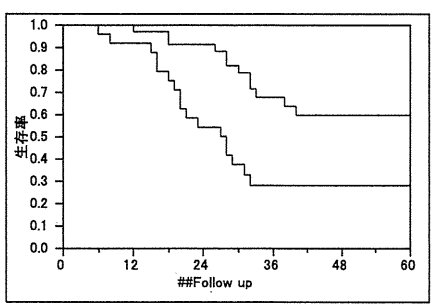

図10. 肺腺癌における予後カーブ(核:青=陽性)

また、肺腺癌では、弱陽性を含めた群を陽性と認識すると、clone 1CBE6-3と同様に核における発現が予後良好因子として認識された(P<0.001)。

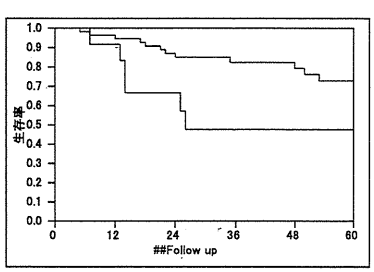

図11. 大腸癌の予後カーブ(核:青=陽性)

興味深いことに大腸がんでは、核の発現が予後不良因子として認識された(P=0.02)。癌腫により機能が異なる可能性を示した。

<Clorf56の染色結果>

染色性は、上皮細胞特にがん細胞の細胞質に観察された 。

図2： Clorf56の免疫染色

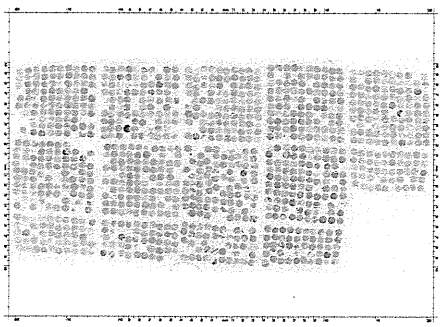

図12. 多種癌の組織アレイにおける染色。

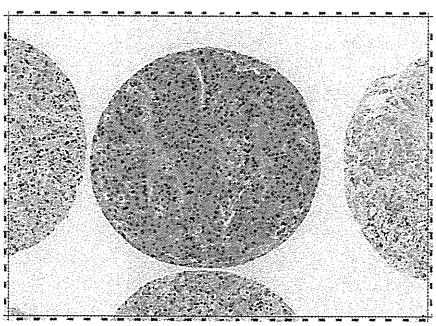

図13. 染色は細胞質に主に観察された。

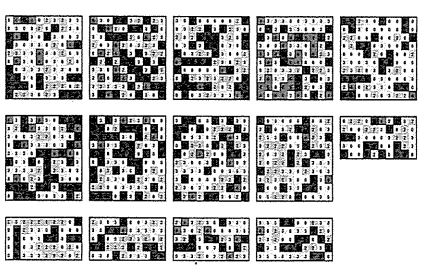

図14. 多種癌における細胞質の発現。

発現は肝臓癌において特に高く観察された。肺腺癌においても比較的高い発現が観察された。

予後との関連性は脳腫瘍、多種癌ともに確認されなかったが、腺がんでは、血管侵襲と負の相関を示した(P=0.021)。また、胃が

んでは、リンパ節転移と負の相関がみられ(P=0.002)、またリンパ管侵襲とも強い負の相関を認めた(P<0.001)。肝癌では、他臓器転移と負の相関がみられ(P=0.014)、膵癌においてもリンパ節転移との負の相関を認めた(P=0.009)。

3）FSTL における染色

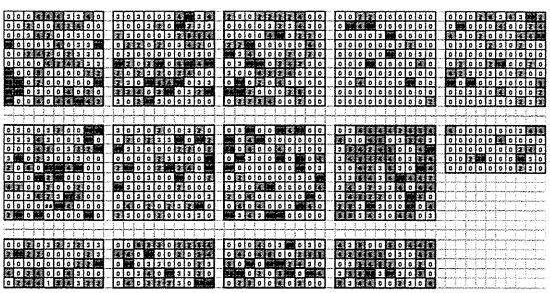

図１５ 多種癌における核内発現

発現は大腸癌と子宮体部癌において強く観察された。予後との相関はいずれの癌腫においても見られなかった。ただし、胃癌では、分化度との正の相関がみられ(P=0.001)、胆道系癌では、他臓器転移と負の相関がみられた(P= 0.04)。

D. 考察

SST クローン免疫法によるモノクローナル抗体作製は順調に進んでいるが、ホルマリン固定、パラフィン包埋された組織における染色に使用できるモノクローナル抗体の作製は困難であり、19 種類のクローンから、特異的な染色性が確認され、最終的に組織アレイへの検討が可能であったものは 2 つの抗原に対する 3 クローンであった。EphA2 では、肺がんにおいて２クローンともに予後良好の因子として認識されたが、大腸癌では予後不良因子として認識された。Clorf56 では、予後との関連性は見られず、肺腺癌、胃癌、肝癌、膵癌において腫瘍の増殖と負の相関を示した。

抗腫瘍効果を示す抗体のターゲットとする分子の機能が腫瘍の進展を抑制することは一見矛盾している様にも感じられる。抗体は単純にたんぱくの機能を抑制することで抗腫瘍効果を示す訳では無い可能性が考えられる。

E. 結論

本年度は最終年として、SST-REX 法により確立された SST クローンから精製された抗体の発現を多種の腫瘍組織にて検討した。SST-REX 法は比較的効率良くパラフィン包埋組織への染色に応用可能なモノクローナル抗体を作製することができた。これらの分子の機能を解析すると、そのいくらかは腫瘍の進展を抑える役割をしている事がわかった。

G. 研究発表

原著論文

1. Zhang C, Elkahloun AG, Robertson M, Gills JJ, Tsurutani J, Shih JH, Fukuoka J, Hollander MC, Harris CC, Travis WD, Jen J, Dennis PA
Loss of cytoplasmic CDK1 predicts poor survival in human lung cancer and confers chemotherapeutic resistance. PLoS One. 6(8):1-15, 2011.

2. Turner BM, Cagle PT, Sainz IM, Fukuoka J, Shen SS, Jagirdar J.

Napsin A, a new marker for lung adenocarcinoma, is complementary and more sensitive and specific than thyroid transcription factor 1 in the differential diagnosis of primary pulmonary carcinoma: evaluation of 1674 cases by tissue microarray.
Arch Pathol Lab Med. 136(2):163-71, 2012

3. Whithaus K, Fukuoka J, Prihoda TJ, Jagirdar J. Evaluation of napsin A, cytokeratin 5/6, p63, and thyroid transcription factor 1 in adenocarcinoma versus squamous cell carcinoma of the lung. Arch Pathol Lab Med. 136(2):155-62, 2012

4. Kanazawa Y, Shojaku H, Takakura H, Fujisaka M, Tachino H, Watanabe Y, Tomizawa G, Kawabe H, Shojaku H, Seto H, Otani K, Fukuoka J, An essential dose of cisplatin for super-selective intra-arterial infusion concomitant with radiotherapy in patient with maxillary squamous cell carcinoma. Eur Arch Oto-phino-l. 10.1007/s00405-011-1857-7O 2011

5. Shibata-Minoshima F, Oki T, Doki N, Nakahara F, Kageyama S, Kitaura J, Fukuoka J, Kitamura T. Identification of RHOXF2 (PEPP2) as a cancer-promoting gene by expression cloning. Int J Oncol. 40(1): 93-8, 2012

6. Fukuoka J, Hofer MD, Hori T, Tanaka T, Ishizawa S, Nomoto K, Saito M, Uemura T, Chirieac LR Spiral Array. A New High-Throughput Technology Covers Tissue Heterogeneity. Arch Pathol Lab Med. 2012: in press

7. Farris, AB III, Demicco EG, Le LP, Finberg KE, Miller J, Mandal R, Fukuoka J, Cohen C, Gaissert HA, Zukerberg LR, Lauwers GY, Iafrate. AJ, Mino-Kenudson, M.
Clinicopathologic and Molecular Profiles of Microsatellite Unstable
Barrett Esophagus-associated
Am J Surg Pathol 2011 in press

8. E G Demicco, A B Farris, Y Baba, B A-Etang, K Bergethon1, Mandal, D Daives, J Fukuoka, M Shimizu, D D-Santagata, S Ogino, A J Iafrate, H A Gaissert, M M -Kenudson.
The Dichotomy in Carcinogenesis of the Distal Esophagus and Esophagogastric Junction: Intestinal-Type vs. Cardiac-Type Mucosa-Associated Adenocarcinoma.
Modern Pathology, 2011, in press.

9. Nagata T, Shimada Y, Sekine S, Hori R, Matsui K, Okumura T, Sawada S, Fukuoka J, Tsukada K.
Prognostic significance of NANOG and KLF4 for breast cancer.
Breast Cancer. DOI.10.1007 /s12282-012-0357-y, 2012

症例報告

1．岡澤成祐，河岸由紀男，猪又峰彦，山田徹，三輪敏郎，林 龍二，松井祥子，菓子井達彦，土岐善紀，長田啓史，福岡順也，戸邉一之

肺過誤腫を合併した若年発症肺癌の１例
日呼吸会誌 2011 49(5):349-354,2011

2 . Nishimizu T, Minemura M, Kajiura S, Tokimitsu Y, Itaya Y, Yamawaki, H,Kawai K, Tajiri K, Nakayama Y, Hosokawa A, Takahara T, Yasumura S, Shimizu S, Fukuoka J, Ishizawa S, Sawasaki T, Yanagisawa A, Sugiyama T. [A case of pancreatic acinar cell carcinoma with a giant liver metastasis successfully treated with combination of gemcitabine and peroral s-1]
癌と化学療法, 38(2): 309-12, 2011.

総説

なし

学会発表

1．福岡順也．「肺癌の病理における最近の話題 」兵庫医科大学大学院特別講義 2011, 02, 兵庫

2. 福岡順也．「肺癌の個別化医療と組織型診断」第 26 回京滋肺癌研究会 2011, 02, 京都

3. Whithaus K, Fukuoka J, Jagirdar J. Evaluation of Napsin A, CK 5/6, p63, nd TTF-1 in Adenocarcinoma (ACA) vs. Squamous Cell Carcinoma (SCC) of the Lung. 100th USCAP Annual meeting, Mar 1-3, 2011, San Antonio, USA

4. Fukuoka J, Sano H, Tanaka T. Central vs. Peripheral Squamous Cell Carcinoma. Are they really different morphologically?. Pulmonary Pathology Society, Biennial Meeting, 2011, 8, 18-20, New York City, USA

5. Fukuoka J, Hori T. Ki-67 is a strong prognostic marker for NSCLC when tissue heterogeneity is considered. 101th USCAP Annual meeting, Mar 19-21, 2011, Vancouver, Canada

6.Sano H, Tanaka T, Saito M, Otani K, Hori T, Nunomura S, Fukuoka J. Difference of morphology and molecular expression between central and peripheral squamous cell carcinoma 101th USCAP Annual meeting, Mar 19-21, 2011, Vancouver, Canada

7.Arora K, Zhang W, Fukuoka J, Kitano H, Jagirdar J. Detection of EGFR mutations in lung adenocarcinoma by immunohistochemistry using mutant specific antibodies: Are we there yet? 101th USCAP Annual meeting, Mar 19-21, 2011, Vancouver, Canada

研究成果の刊行に関する一覧表

雑誌

発表者氏名	論文タイトル名	発表誌名	巻号	ページ	出版年
Shibata-Minoshima, F	Identification of RHOXF2 (PEPP2) as a cancer-promoting gene by expression cloning.	Int J Oncology	40	93-98	2012
Kato, N	Two types of C/EBPa mutations play distinct roles in leukemogenesis: Lessons from clinical data and BMT models.	Blood	117	221-233	2011
Turner, BM	Napsin A, a new marker for lung adenocarcinoma, is complementary and more sensitive and specific than thyroid transcription factor 1 in the differential diagnosis of primary pulmonary carcinoma: evaluation of 1674 cases by tissue microarray.	Arch Pathol Lab Med	136	163-171	2012

Identification of RHOXF2 (PEPP2) as a cancer-promoting gene by expression cloning

FUMI SHIBATA-MINOSHIMA[1,2*], TOSHIHIKO OKI[1,2*], NORIKO DOKI[1,2], FUMIO NAKAHARA[1,2], SHUN-ICHIRO KAGEYAMA[3], JIRO KITAURA[1,2], JUNYA FUKUOKA[3] and TOSHIO KITAMURA[1,2]

Divisions of [1]Cellular Therapy and [2]Stem Cell Signaling, the Institute of Medical Science, the University of Tokyo, 4-6-1 Shirokanedai, Minatoku, Tokyo 108-8639; [3]Department of Surgical Pathology, Toyama University, 2630 Sugitani, Toyama 930-0194, Japan

Received June 27, 2011; Accepted July 28, 2011

DOI: 10.3892/ijo.2011.1173

Abstract. Multiple mutations contribute to establish cancers. We have searched for potential oncogenes by screening cDNA libraries derived from gastric cancer cell lines, pancreatic cancer cell lines and glioma cell lines, using retrovirus-mediated expression cloning. Two types of interleukin-3 (IL-3)-dependent cell lines, Ba/F3 and HF6, were transduced with the cDNA libraries and several genes that render these cells factor-independent were identified including *PIM-1*, *PIM-2*, *PIM-3*, *GADD45B* and reproductive homeobox genes on the X chromosome gene F2 (*RHOXF2*). Although no mutation in these genes was found, these molecules were highly expressed in cancer cell lines and they may play important roles in cell transformation. Among them, we focused on a transcriptional repressor RHOXF2. Transduction of RHOXF2 rendered HF6 cells factor-independent, while knockdown of RHOXF2 inhibited growth of the HGC27 gastric cancer cell line which highly expresses RHOXF2. In addition, RHOXF2-transduced HF6 cells quickly induced leukemia when transplanted into sublethally irradiated mice. Moreover, RHOXF2 is highly expressed in some leukemia cell lines and a variety of human cancer samples including colon and lung cancers. Thus, these results indicate that RHOXF2 is involved in carcinogenesis.

Introduction

Cancer develops through a multistep process involving a variety of gene alterations and epigenetic changes (1,2). Genes that are commonly altered include Rb, $p16^{INK4a}$, VHL, Ras, p53 and APC (2,3). Fusion genes resulting from chromosomal translocations are established hallmarks of hematopoietic malignancies and include BCR-ABL, MLL-fusions and AML1-ETO (6). More recently, fusion genes have also been identified in solid tumors, for example EML4-ALK in lung cancer (4), EWS-FLI-1 in Ewing's sarcoma (5) and ETV6-NTRK3 in fibrosarcoma and breast cancer (6). Oncogenic mutations were originally identified using transfected NIH3T3 cells (7) in the focus-forming assay. A combination of the focus-forming assay with inoculation of NIH3T3 cells *in vivo* later increased the sensitivity to detect oncogenic potential (8). Recently, Soda *et al* identified a fusion gene EML4-ALK in non-small cell lung cancer by retrovirus-mediated expression cloning using transformation of the NIH3T3 cells as an assay (4). EML4-ALK is now a promising molecular therapeutic target; ALK inhibitors proved to be effective in the therapy for non-small cell lung cancer patients bearing this fusion gene (9). Detection of oncogenes has largely depended on the classical focus-forming assay with NIH3T3, which mainly detects activated mutations of Ras and gene alterations that activate the Ras pathway (7). To detect different classes of oncogenic mutations, different assays are likely to be required.

In this study, two hematopoietic cell lines, Ba/F3 (10) and HF6 (11), were used to search for potential oncogenes in several cancer types. Both cell lines are interleukin-3 (IL-3)-dependent early myeloid cells, but to become factor-independent, Ba/F3 requires JAK-STAT signaling and HF-6 requires Ras activation (11-13). Genes were tested for the ability to render these cell lines factor-independent. Using this strategy, several genes from cDNA libraries of gastric cancer cell lines, pancreatic cancer cell lines and glioma cell lines were identified including *PIM-1*, *PIM-2*, *PIM-3*, *GAD45B* and *RHOXF2*. Although mutations in these genes were not found, overexpression of *PIM-1*, *PIM-2*, *PIM-3*, *GAD45B* and *RHOXF2* rendered HF6 cells factor-independent, confirming the validity of the functional screening. Of the genes identified, we have focused on a homeobox protein, reproductive homeobox genes on the X chromosome F2 (RHOXF2), also known as PEPP2. Homeobox proteins, share a DNA-binding homeodomain motif of 60 amino acids, and are transcription factors that regulate development. The Rhox genes belong to a recently discovered homeobox family whose members are clustered on the X chromosome (14-16). Whereas the human RHOX family consists of three members, RHOXF1, RHOXF2 and RHOXF2B, the murine

Correspondence to: Dr Toshio Kitamura, Division of Cellular Therapy, the Institute of Medical Science, the University of Tokyo, 4-6-1 Shirokanedai, Minatoku, Tokyo 108-8639, Japan
E-mail: kitamura@ims.u-tokyo.ac.jp

*Contributed equally

Key words: c-DNA library screening, factor-independent growth, homeobox gene

Rhox family consists of >30 members (14-16). Rhox proteins are expressed in germ cells, embryonic cells and somatic cells of reproductive tissue, and play important roles in embryonic, postnatal and adult development, especially of the male and female reproductive systems. Recently, human and mouse Rhox protein expression in some cancer cells including breast and colon cancer was reported (16), and expression of a mouse Rhox family member, Rhox5, was found in 50-65% of cancer cells (17,18). Interestingly, Rhox protein expression is regulated by epigenetic mechanisms, and the treatment with DNA methyltransferase inhibitors, such as decitabine, induces Rhox expression (16). These findings indicate that Rhox proteins are involved in carcinogenesis. In the present study, it was found that knockdown of RHOXF2 attenuated the growth of a gastric cancer cell line HGC27 and overexpression of RHOXF2 in HF6 cells rapidly induced leukemia in transplanted mice. These results support a role for RHOXF2 in cell transformation.

Materials and methods

Cells. Human gastric cancer cell lines (HGC27, GCIY, KATOIII, MKN45, OCUM-1, AGS, MKN1, MKN7, MKN45, MKN74, NUGC3, SNU719, TMK-1), human pancreatic cancer cell lines (Bx-PC-3, AsPC-1, capan1) and human glioma cell lines (U87MG, T98G, U251) were maintained in Dulbecco's modified Eagle's medium (DMEM) supplemented with 10% fetal calf serum (FCS). Ecotropic and amphotropic retrovirus packaging cell lines, PLAT-E and PLAT-A respectively, were maintained in DMEM supplemented with 10% FCS, 1 μg/ml puromycin and 10 μg/ml blasticidin (19). A murine pro-B cell line Ba/F3 was maintained in RPMI-1640 with 10% FCS and 1 ng/ml mouse IL-3 (mIL-3), and a murine myelomonocytic cell line HF6 was maintained in RPMI-1640 with 20% FCS and 10 ng/ml mIL-3 (11).

Plasmids and primers. The coding region of RHOXF2 was amplified from HGC27 cDNA by PCR using Phusion polymerase (Finnzymes, Oy, Finland), then subcloned into pMXs-puro or pMXs-IG vectors (19,20) and the sequence was confirmed. Primers for RHOXF2 used in RT-PCR were as follows; (forward primer: cggaccagtgtagccagtat; reverse primer: tgacctcttcagtaagcgaca).

To generate shRNA vectors, first two oligonucleotides were designed using the siRNA Target Finder (Ambion Inc., Austin, USA) and were synthesized as follows; RHOXF2-1 (sense: ggca cagcagcaggagaaa, antisense: tttctcctgctgctgtgcc) and RHOXF2-2 (sense: gagccaaatggaggagaca, antisense: tgtctcctccatttggctc). These oligonucleotides were annealed and ligated to the pReps vector, which was kindly provided by T. Hara (21). Control shLuc vector targeting firefly luciferase was constructed in the same way.

Generation of anti-RHOXF2 antibody. Anti-RHOXF2 polyclonal antibody was generated from the serum of rabbits immunized with the purified GST-RHOXF2 fusion protein (Scrum Inc., Tokyo, Japan).

Retroviral gene transduction. Retroviral transduction was performed as described (19,20). Briefly, ecotropic and amphotropic retroviruses were generated by the packaging cell lines Plat-E and Plat-A, respectively, and then transiently transfected with a pMXs-based construct using FuGENE 6 reagent (Roche Applied Science, Basel, Switzerland). Two days after transfection, ecotropic and amphotropic retroviruses were collected and used to infect mouse HF6 cells or human HGC27 cells, respectively.

Screening of cDNA libraries. pMXs-based cDNA libraries were generated from gastric cancer cell lines, pancreatic cancer cell lines and glioma cell lines, as previously described (13). Each cDNA library was retrovirally introduced into two IL-3-dependent cell lines, Ba/F3 and HF6. Two days after transduction, the cells were seeded into 96-well plates in the absence of IL-3 in order to select factor-independent clones. To identify the cDNA that conferred Ba/F3 or HF6 cells with factor-independency, the integrated cDNAs were isolated from factor-independent clones by genomic PCR and were sequenced using primers specific to the retroviral vector sequence.

Soft agar colony formation. One thousand cells were suspended in 0.6% agar supplemented with complete culture medium. This suspension was layered over 1.2% agar-medium bottom layer in 35-mm dishes. After 14 days, colonies were counted.

Mouse bone marrow transplantation (BMT). One million HF6 cells transduced with empty (mock) or RHOXF2-containing retroviral vector were injected into the tail vein of sub-lethally irradiated (5.25 Gy) C57BL/6 (Ly-5.1) 8-week-old mice. Overall survival of the transplanted mice was analyzed using the Kaplan-Meier method. Animal studies were conducted in according to the guidelines of the Animal Care Committee at the Institute of Medical Science, University of Tokyo.

Generation of tissue microarray. Tissue microarrays (TMA) were generated from 1150 cases of 14 common cancer types as previously described (22). In addition, TMA composed of 280 non-neoplastic adjacent tissues from the same patients were made using identical methods. Each sample of TMA was cut in 4-μm section for immunohistochemical analysis. Tissue microarray methods in the present study were approved by the Ethics Committee of Toyama University (no. 19-12).

Immunohistochemical analysis of tissue microarrays. Immunohistochemical detection of RHOXF2, and statistical analyses of results were carried out as previously described (22). In short, after deparafinization and rehydration, sections were processed for heat-induced antigen retrieval at 125°C and incubated with diluted antibody (1:500) for 30 min at room temperature. Antibody staining was visualized using the Envision$^+$ system (Dako, Kyoto, Japan) and diaminobenzidine.

Nuclear staining was scored according to 4 grades (0, none; 1, mild; 2, moderate; 3, marked). Scores 0 and 1 were considered negative while scores 2 and 3 were considered positive. RHOXF2 staining of sections of an embedded pellet of HF6 cell line and colonic mucosa were used as positive and negative staining controls, respectively (data not shown).

Results

Expression cloning of potential oncogenes from cancer cell lines. cDNA was generated from gastric cancer cell lines,

Table I. Characteristics of c-DNA libraries.

	Gastric Cancer	Pancreatic cancer	Glioma
Cell lines	HGC-27, OCUM-1, MKN45, GCIY, KATOIII	BxPC-3, AsPC-1, capan1	U87MG, T98G, U251
Library size	$4.5x10^6$	$3x10^6$	$3x10^6$
Avarage length of cDNAs (kb)	1.2	1.4	1.3

The name of the cell lines used for making each library (cell lines), the numbers of independent cDNA clones of each library (library size), and the average length of the cDNAs included in each library (avarage length of cDNAs) are described.

Table II. Details of the isolated clones from screening.[a]

	Gastric	Pancreatic	Glioma
Total isolated clone	5	2	6
The clones with full ORF	*PIM-1,3, RNF67, RHOXF2*	*PIM-1, GADD45B*	*PIM-2,3, CSF3, GADD45B*
The clones with partial ORF	*TENC1, RAF1*		*FOXM1, ATXN1*
The candidate oncogenes	*PIM-1,3, RHOXF2*	*PIM-1, GADD45B*	*PIM-2,3, GADD45B*

[a]The clones isolated from 3 different c-DNA libraries are shown. The clones consist of two categories, the clones with full length of open reading frame (ORF) of cDNAs (the clones with full ORF) and the clones with partial sequence of ORF (the clones with partial ORF). The names of the genes which the clones of each category from 3 kinds of libraries contain, are shown in the table. Among the genes from the clones with full length ORF, some genes rendered HF6 factor-independent and the names of the genes are indicated in the table (the candidate oncogenes).

pancreatic cancer cell lines and glioma cell lines as described, and a cDNA library was constructed from the mixed cDNAs from each cancer in a retrovirus vector pMXs (20) (Table I). The resulting library was introduced into IL-3-dependent Ba/F3 cells and HF6 cells via retrovirus infection, and the infected cells were cultured in the absence of IL-3 to identify potential oncogenes that render the cells factor-independent. Several factor-independent clones were established from HF6 transfectants and *PIM-1*, *PIM-2*, *PIM-3*, *GADD45B* and *RHOXF2* were isolated from these clones by genomic PCR (Table II). These genes were introduced into HF6 cells and the ability of these genes to confer HF6 cells with autonomous growth was confirmed (data not shown). However, no mutation was found in these genes, indicating that overexpression of these genes alone could transform HF6 cells.

Expression of RHOXF1 and F2 in a variety of cell lines. The Rhox family consists of 30 members in mice and 3 members in humans, RHOXF1, F2 and F2B. Interestingly, expression of RHOXF1 and F2 was almost mutually exclusive in gastric cancer cells examined (Fig. 1A). HGC27 (undifferentiated carcinoma), NUGC3 (poorly differentiated adenocarcinoma) and TMK-1 (poorly differentiated adenocarcinoma) cell lines express RHOXF2 but not RHOXF1. On the other hand, GCIY (scirrhous), MKN1 (adeno-squamous), MKN7 (well differentiated adenocarcinoma), MKN74 (moderately differentiated adenocarcinoma) and SNU719 (well differentiated adenocarcinoma) cell lines express RHOXF1 but not RHOXF2. These results suggested complementary roles for RHOXF1 and F2.

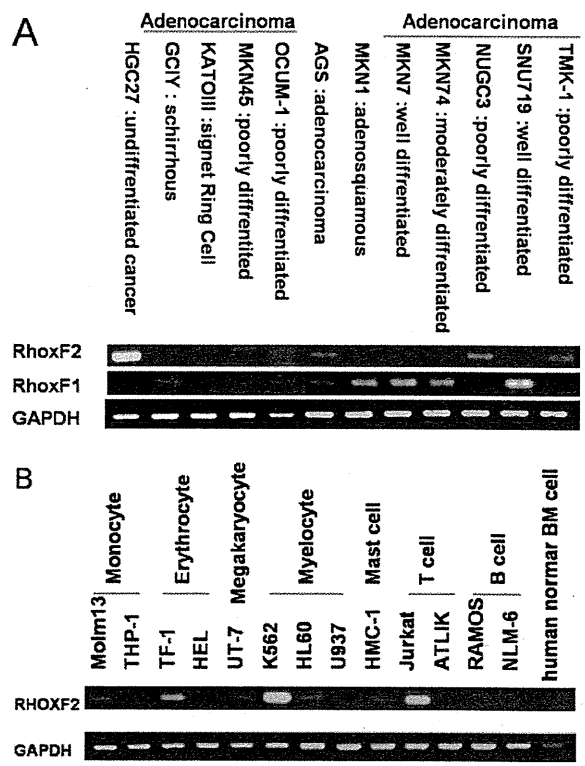

Figure 1. Expression of RHOXF2 in cancer cell lines. Expression of RHOXF2 was analyzed by RT-PCR. The expression in gastric cancer cell lines (A) and cell lines derived from hematological malignancies (B) are shown.

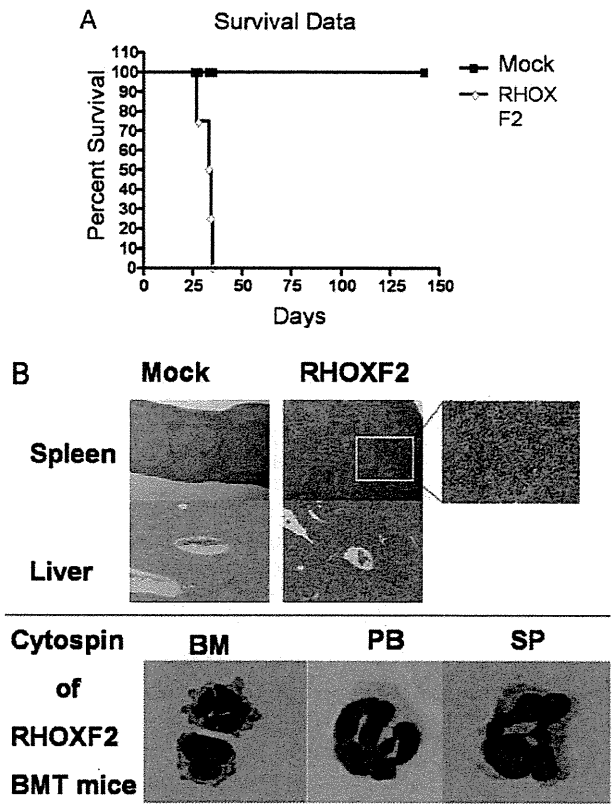

Figure 2. Leukemia-like disease was induced by HF6 transduced with RHOXF2 but not by parental HF6 cells. The effects of RHOXF2 overexpression were analyzed using a mouse BMT model. Kaplan-Meier survival curves for mice transplanted with HF6-mock cells (black squares) or HF6-RHOXF2-transfectants (white diamonds) are shown (A). Hematoxylin & eosin-stained histological samples and May-Giemsa-stained cytospins revealed that hepato-splenomegaly caused by a leukemia-like cell infiltration was observed in mice transplanted with HF6-RHOXF2-trasnfectants (B).

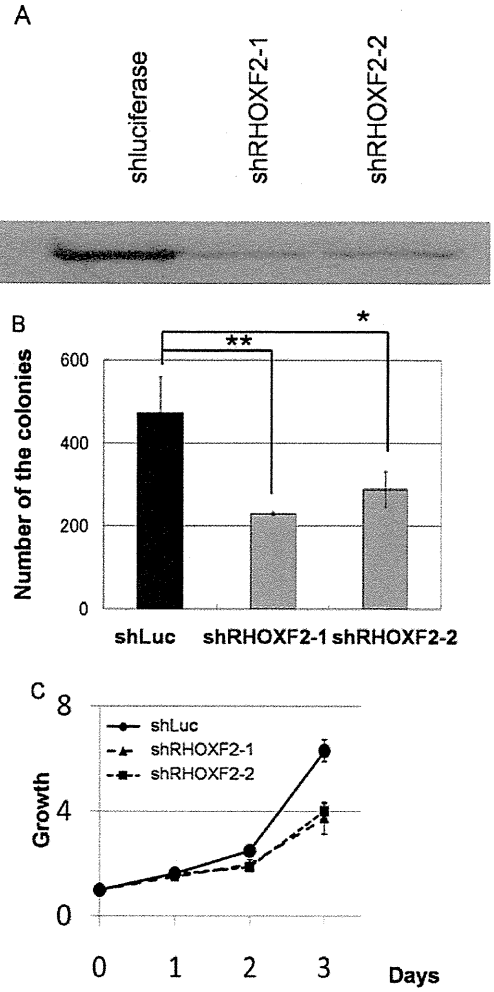

Figure 3. Knockdown of RHOXF2 attenuated the growth of a gastric cancer cell line, HGC27. Two shRNA vectors, shRHOXF2-1 and shRHOXF2-2, were designed to knockdown RHOXF2. Both shRNAs effectively inhibited the expression of RHOXF2 protein (A). shLuciferase vector was used as a control (shLuc). Colony formation in soft agar (B) and cell growth (C) of HGC27 transfectants were inhibited by shRHOXF2-1 (squares) and shRHOXF2-2 (triangles) but not by shLuc (circles). Statistical analysis was performed using the t-test; $^{*}P<0.05$, $^{**}P<0.01$. All experiments were conducted in triplicates. The result shown here is a representative of 3 independent experiments.

The undifferentiated to poorly differentiated gastric cancers tended to express RHOXF2, while the adenocarcinoma cell line AGS appeared to express both RHOXF1 and F2.

RHOXF2 was also highly expressed in the human immature leukemic cell lines including TF-1 and K562 (Fig. 1B). It was also expressed in the other human hematopoietic cell lines, MOLM13, UT-7, HL60, MHC-1 and Jurkat (Fig. 1B).

Effects of overexpression of RHOXF2 in HF6 cells. HF6 cells that were manipulated to express RHOXF2 proliferated autonomously *in vitro* in the absence of IL-3 (data not shown). Next the effects of RHOXF2 overexpression *in vivo* were examined using a mouse BMT model. While unmanipulated HF6 cells did not induce disease in 5 months after the transplantation into sub-lethally irradiated mice, HF6 cells expressing RHOXF2 rapidly induced leukemia-like disease (Fig. 2A). In these mice, the leukemic cells infiltrated to the liver and spleen, causing hepato-splenomegaly (Fig. 2B).

Effects of RHOXF2 knockdown in HGC27. Next, the effects of RHOXF2 knockdown were evaluated. To achieve this, shRNA specific for RHOXF2 was retrovirally introduced into HGC27 gastric cancer cells which express RHOXF2 at high levels (Fig. 3A). While the control shLuciferase did not inhibit the expression of RHOXF2, two RHOXF2 sh-RNA constructs efficiently suppressed the expression of RHOXF2 in HGC27 cells (Fig. 3A). Knockdown of RHOXF2 inhibited the colony forming ability of HGC27 cells in soft agar (Fig. 3B) and the growth rate in a liquid culture (Fig. 3C), implicating RHOXF2 in transformation and cell growth.

Expression of RHOXF2 in a multi-cancerous tissue microarray. Expression of RHOXF2 in a variety of cancers and non-neoplastic tissues was evaluated using two TMA blocks (Fig. 4). RHOXF2 was not highly expressed in any of the normal tissues tested except for thyroid. RHOXF2 was highly expressed in some of the cancers including lung squamous cell carcinoma, thyroid tumors, colon, breast, gastric, prostate, ovarian and uterine corpus cancers.

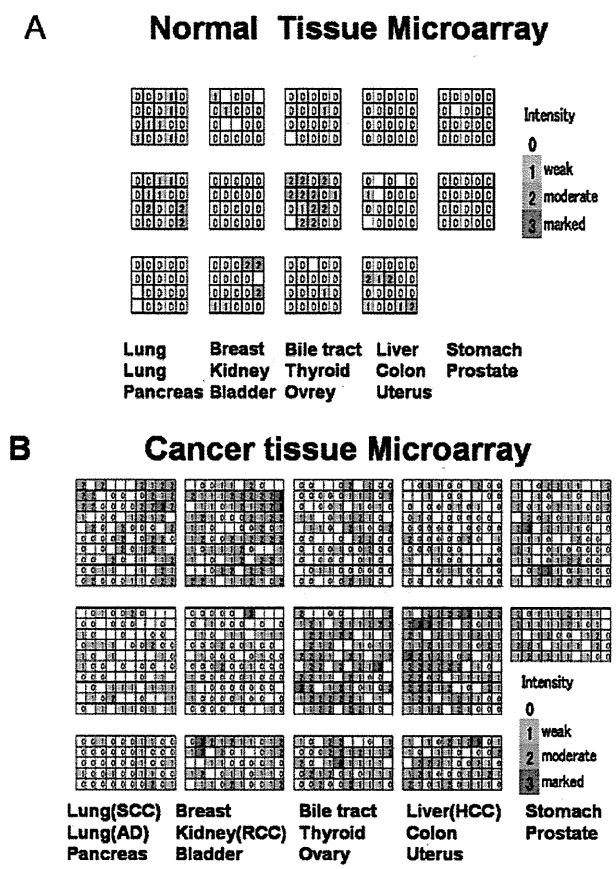

Figure 4. Tissue microarray analysis. Immunohistochemical analysis of RHOXF2 expression in multi-tissue array is shown. (A and B) The array contains 280 non-neoplastic tissue samples and 1150 tumor tissue samples from 14 major types of cancers. Each column represents each case and the number in the column indicates the score corresponding to the level of RHOXF2 expression.

Discussion

In the present work, a transcriptional repressor RHOXF2 has been identified as a potential oncogene by functional expression cloning. Knockdown of RHOXF2 inhibited the growth and colony forming ability of the gastric cancer cell line HGC27. On the other hand, overexpression of RHOXF2 conferred IL-3-dependent HF6 cells with autonomous growth and leukemogenicity *in vivo*. In addition, RHOXF2 expression was found in a variety of cancer tissues. Recently, several studies have reported that expression of RHOXF2 is regulated by some epigenetic mechanisms, especially in cancer tissues (16). These findings suggest that RHOXF2 plays a role in tumorigenesis and that it can be controlled epigenetically. To elucidate the molecular mechanisms, further studies using gene chips and bioinformatics are required to identify the responsive genes downstream of RHOXF2. HF6 is a mouse bone marrow-derived IL-3-dependent cell line immortalized by the fusion gene MLL-SEPT6, and activation of the Ras pathway in these cells can lead to transformation (11,13). Ras activation frequently plays an important role in carcinogenesis and it is possible that genes repressed or enhanced by RHOXF2 are involved in this pathway.

It is now recognized that as in solid tumors, multiple mutations are involved in the development of hematopoietic malignancies. These mutations are classified into two groups; class I mutations include activating mutations of tyrosine kinases and oncogenes, and inactivating mutations of tumor suppressor genes such as p53, NF1, while class II mutations include dominant-negative mutations of transcription factors and chromatin modification enzymes (23-25). We have previously demonstrated that a class II mutation MLL-SEPT6 could immortalize mouse bone marrow cells by blocking the differentiation of hematopoietic progenitors (11-13). However, these immortalized cells still require interleukin 3 (IL-3) for their growth. Interestingly, class I mutations such as those that activate Ras signal or constitutively active receptors tyrosine kinase mutants, like FLT3-ITD, were able to fully transform the IL-3-dependent HF6 cells immortalized by class II mutations (13).

The assay system using NIH3T3 cells has been the gold standard for screening of oncogenes, however this system mainly detects activators of the Ras pathway (7). For this reason, different cell types have been needed to be tested in the search for the oncogenic mutations. In the present study, HF6 cells and Ba/F3 cells were used. HF6 cells and Ba/F3 cells require activation of the Ras pathway and the JAK-STAT pathway, respectively, for the full transformation. In addition, we have established a cell line HF8 cells by introducing Hes1 to bone marrow progenitors. Neither Ras nor JAK/STAT activation could confer HF8 cells with autonomous growth (unpublished observation), indicating that these IL-3-dependent cell lines examined have distinct signaling profiles. The use of different cell lines could therefore, identify different classes of mutations. In the present study, *PIM-1*, *PIM-2*, *PIM-3*, *GADD45B* and *RHOXF2* were shown to render HF6 cells factor-independent, demonstrating the potential for using cells of hematopoietic origin to identify oncogenic mutations. It is possible that different types of mutations and translocations could be identified, using distinct types of IL-3-dependent cell lines.

In conclusion, the transcriptional repressor RHOXF2 is expressed in a variety of cancers, and plays a critical role in tumorigenesis. The use of IL-3-dependent cell lines for screening cDNA libraries has potential as a strategy in the search for oncogenes.

Acknowledgements

We thank Dr T. Hara for kindly providing the retrovirus shRNA vector (pReps), and Mr. Masunori Kajikawa, ACTGen Inc., (Komagane, Japan) for providing cancer cell lines. This work was supported by grants from the Ministry of Health, Labor and Welfare.

References

1. Hanahan D and Weinberg RA: The hallmarks of cancers. Cell 100: 57-70, 2000.
2. Esteller M: Epigenetics in cancer. N Eng J Med 358: 1148-1159, 2008.
3. Jones PA and Baylin SB: The fundamental roles of epigenetic events in cancer. Nat Rev Genet 3: 415-428, 2002.
4. Soda M, Choi YL, Enomoto M, *et al*: Identification of the transforming EML4-ALK fusion gene in non-small-cell lung cancer. Nature 448: 561-566, 2007.

5. Delattre O, Zucman J, Plougastel B, *et al*: Gene fusion with an *ETS* DNA-binding domain caused by chromosome translocation in human tumours. Nature 359: 162-169, 1992.
6. Mitelman F, Johansson B and Mertens F: Fusion genes and rearranged genes as a linear function of chromosome aberration in cancer. Nat Genet 36: 331-334, 2004.
7. Clark GL, Cox AD, Graham SM and Der CJ: Biological assays for Ras transformation. Method Enzymol 255: 395-412, 1995.
8. Takahashi K, Mitsui K and Yamanaka S: Role of ERas in promoting tumour-like properties in mouse embryonic stem cells. Nature 423: 541-545, 2003.
9. Gerber DE and Minna JD: ALK inhibition for non-small cell lung cancer: from discovery to therapy in record time. Cancer Cell 18: 548-551, 2010.
10. Palacios R and Steinmetz M: IL3-dependent mouse clones that express B-220 surface antigen, contain ig genes in germ-line configuration, and generate B lymphocytes in vivo. Cell 41: 727-734, 1985.
11. Ono R, Nakajima H, Ozaki K, *et al*: Dimerization of MLL fusion proteins and FLT3 activation synergize to induce multiple-lineage leukemogenesis. J Clin Invest 115: 919-929, 2005.
12. Onishi M, Nosaka T, Misawa K, *et al*: Identification and characterization of a constitutively active STAT5 mutant that promotes cell proliferation. Mol Cell Biol 18: 3871-3879, 1998.
13. Watanabe-Okochi N, Oki T, Komeno Y, *et al*: Possible involvement of RasGRP4 in leukemogenesis. Int J Hematol 89: 470-481, 2009.
14. Maclean JA II, Chen MA, Wayne CM, *et al*: Rhox: a new homobox gene cluster. Cell 120: 369-382, 2005.
15. MacLean JA II and Wilkinson MF: The Rhox genes. Reproduction 140: 195-213, 2010.
16. Li Q, Bartlett DL, Gorry MC, O'Malley ME and Guo ZS: Three epigenetic drugs up-regulate homeobox gene Rhox5 in cancer cells through overlapping and distinct molecular mechanisms. Mol Pharmacol 76: 1072-1081, 2009.
17. Wilkinson MF, Kleeman J, Richards J and MacLeod CL: A novel oncofetal gene is expressed in a stage-specific manner in murine embryonic development. Dev Biol 141: 451-455, 1990.
18. Ono T, Sato S, Kimura N, *et al*: Serological analysis of BALB/C methylcholanthrene sarcoma Meth A by SEREX: identification of a cancer/testis antigen. Int J Cancer 88: 845-851, 2000.
19. Morita S, Kojima T and Kitamura T: Plat-E: an efficient and stable system for transient packaging of retroviruses. Gene Ther 7: 1063-1066, 2000.
20. Kitamura T, Koshino Y, Shibata F, *et al*: Retrovirus-mediated gene transfer and expression cloning: powerful tools in functional genomics. Exp Hematol 31: 1007-1014, 2003.
21. Fujino RS, Tanaka K, Morimatsu M, Tamura K, Kogo H and Hara T: Spermatogonial cell-mediated activation of an IκBζ-independent nuclear factor-κB pathway in sertoli cells induces transcription of the lipocalin-2 gene. Mol Endcrinol 20: 904-905, 2006.
22. Kitano H, Kageyama S, Hewitt SM, *et al*: Podoplanin expression in cancerous stroma induces lymphangiogenesis and predicts lymphatic spread and patient survival. Arch Pathol Lab Med 134: 1520-1527, 2010.
23. Gilliland DG: Molecular genetics of human leukemias: new insights into therapy. Semin Hematoi 39: 6-11, 2002.
24. Dash A and Gilliland DG: Molecular genetics of acute myeloid leukaemia. Best Pract Res Clin Haematol 14: 49-64, 2001.
25. Renneville A, Roumier C, Biggio V, *et al*: Cooperating gene mutations in acute myeloid leukemia: a review of the literature. Leukemia 22: 915-993, 2003.

Two types of C/EBPα mutations play distinct but collaborative roles in leukemogenesis: lessons from clinical data and BMT models

Naoko Kato,[1,2] Jiro Kitaura,[1] Noriko Doki,[1] Yukiko Komeno,[1] Naoko Watanabe-Okochi,[3] Katsuhiro Togami,[1] Fumio Nakahara,[1,2] Toshihiko Oki,[1,2] Yutaka Enomoto,[1] Yumi Fukuchi,[4] Hideaki Nakajima,[4] Yuka Harada,[5] Hironori Harada,[6] and Toshio Kitamura[1,2]

Divisions of [1]Cellular Therapy and [2]Stem Cell Signaling, Institute of Medical Science, University of Tokyo, Tokyo, Japan; [3]Department of Hematology and Oncology, Graduate School of Medicine, University of Tokyo, Tokyo, Japan; [4]Division of Hematology, Department of Internal Medicine, Keio University School of Medicine, Tokyo, Japan; [5]International Radiation Information Center, Research Institute for Radiation Biology and Medicine, Hiroshima University, Hiroshima, Japan; and [6]Department of Hematology and Oncology, Research Institute for Radiation Biology and Medicine, Hiroshima University, Hiroshima, Japan

Two types of mutations of a transcription factor CCAAT-enhancer binding protein α (C/EBPα) are found in leukemic cells of 5%-14% of acute myeloid leukemia (AML) patients: N-terminal mutations expressing dominant negative p30 and C-terminal mutations in the basic leucine zipper domain. Our results showed that a mutation of C/EBPα in one allele was observed in AML after myelodysplastic syndrome, while the 2 alleles are mutated in de novo AML. Unlike an N-terminal frame-shift mutant (C/EBPα-N^m)–transduced cells, a C-terminal mutant (C/EBPα-C^m)–transduced cells alone induced AML with leukopenia in mice 4-12 months after bone marrow transplantation. Coexpression of both mutants induced AML with marked leukocytosis with shorter latencies. Interestingly, C/EBPα-C^m collaborated with an Flt3-activating mutant Flt3-ITD in inducing AML. Moreover, C/EBPα-C^m strongly blocked myeloid differentiation of 32Dcl3 cells, suggesting its class II mutation-like role in leukemogenesis. Although C/EBPα-C^m failed to inhibit transcriptional activity of wild-type C/EBPα, it suppressed the synergistic effect between C/EBPα and PU.1. On the other hand, C/EBPα-N^m inhibited C/EBPα activation in the absence of PU.1, despite low expression levels of p30 protein generated by C/EBPα-N^m. Thus, 2 types of C/EBPα mutations are implicated in leukemogenesis, involving different and cooperating molecular mechanisms. (*Blood.* 2011; 117(1):221-233)

Introduction

The CCATT/enhancer binding protein α (C/EBPα) transcription factor is a critical regulator of proliferation and differentiation in myeloid cells.[1,2] C/EBPα consists of an N-terminal transcriptional activation domain and a C-terminal basic leucine zipper (bZIP) domain.[3-5] Two isoforms of C/EBPα proteins are generated from different translation start sites: a full-length 42-kDa protein (p42) and a truncated 30-kDa protein (p30) that lacks an N-terminal transcriptional activation domain. C/EBPα-p30 isoform inhibits C/EBPα-p42–mediated transcription.[6-8] Importantly, C/EBPα promotes differentiation both by up-regulation of lineage-specific gene products[9-11] and by proliferation arrest.[12] Recent studies have indicated that C/EBPα-induced growth arrest is regulated by its interaction with other molecules involved in growth control: E2F,[13-15] Max,[16] and SWI/SNF chromatin remodeling complexes.[17] For example, repression of E2F activity by E2F-C/EBPα interaction results in the down-regulation of c-Myc, leading to granulocytic differentiation.[18,19]

According to several studies, *CEBPA* mutations are found in 5%-14% of acute myeloid leukemia (AML) patients belonging to the French-American-British subtypes M1, M2, or in some cases M4.[8,20-22] The mutations of the *CEBPA* gene can be largely categorized into 2 types: one is an N-terminal frame-shift mutation disrupting p42 and producing p30 as a major product, and the other is a C-terminal in-frame mutation disrupting the bZIP region. Interestingly, most AML patients with *CEBPA* mutations have both mutations simultaneously,[23-25] and such patients displayed a favorable outcome.[22,26] On the other hand, AML patients with single *CEBPA* mutations did not express a distinctive signature, presumably due to a variety of associating gene alterations, including Flt3 activating mutations. Related to this, involvement of single *CEBPA* mutations with myelodysplastic syndrome (MDS) remains to be clarified.[27,28]

Analysis of mice with genetic alterations in the *CEBPA* locus has contributed to delineation of molecular mechanisms by which *CEBPA* mutations induce leukemia. Conditional deficiency of C/EBPα led to a differentiation block at the transition between common myeloid progenitors and granulocyte/monocyte progenitors but not to development of leukemia.[1] However, Cebpa$^{L/L}$ mice, expressing only p30 as C/EBPα protein, developed myeloid leukemia with complete penetration.[29] On the other hand, Cebpa$^{BRM2/BRM2}$ mice, carrying a point mutation in the bZIP domain that dampened E2F interaction, showed only preleukemic features.[14] Interestingly, the same group has recently reported combinational effects of the C-terminal and the N-terminal mutations on leukemogenesis by using Cebpa$^{L/L}$ mice, Cebpa$^{K/K}$ mice carrying the K313 duplication in the C-terminal domain, and Cebpa$^{K/L}$ mice.[29,30] They proposed that efficient leukemogenesis is caused by the combination of both premalignant HSC expansion induced by

Submitted February 17, 2010; accepted September 22, 2010. Prepublished online as *Blood* First Edition paper, September 30, 2010; DOI 10.1182/blood-2010-02-270181.

The online version of this article contains a data supplement.

The publication costs of this article were defrayed in part by page charge payment. Therefore, and solely to indicate this fact, this article is hereby marked "advertisement" in accordance with 18 USC section 1734.

C-terminal *CEBPA* mutation and residual myeloid lineage commitment maintained by the N-terminal *CEBPA* mutation.[30]

Causative gene alterations in hematologic malignancies have been extensively studied, and it is now recognized that multiple mutations contribute to development of leukemia. These gene alterations are categorized into 2 groups, class I and class II mutations.[31,32] Class I mutations include activating mutations of *FLT3*, *C-KIT*, *JAK2*, *SHP2*, and *RAS*, or inactivating mutations of *TP53* and *NF-1*, and induce proliferation or block apoptosis of hemopoietic cells. On the other hand, class II mutations disrupt normal functions of transcription factors and chromosome-modifying enzymes including *MLL*, *RUNX1*, *RARA*, and *PU.1* and hamper differentiation of hemopoietic cells. Combinations of class I and class II mutations are frequently observed in patients' leukemic cells.[33,34] In addition, we and others presented evidence that class I and class II mutations collaborate in the development of leukemia in mouse models.[35,36] Among a variety of gene alterations found in leukemia, *CEBPA* mutations are unique because different *CEBPA* mutations are frequently found on different alleles in leukemic cells of de novo AML.[22-26]

In the present study, we searched for mutations of the *CEBPA* gene in patients with myeloid malignancies, and found N- and C-terminal double mutations in patients with de novo AML. In patients with MDS/AML or therapy-related AML or MDS, only N- or C-terminal single mutation was identified. We chose a C-terminal mutation 304_323dup (hereafter called C/EBPα-C^m) and an N-terminal mutation (T60fsX159) (hereafter C/EBPα-N^m) for further analysis that had been isolated as double *CEBPA* mutations in a de novo AML patient. To evaluate the effects of these mutations on leukemogenesis, we used a mouse bone marrow transplantation (BMT) model. Interestingly, unlike the phenotype in $Cebpa^{K/K}$, $Cebpa^{K/+}$, $Cebpa^{BRM2/BRM2}$, or $Cebpa^{BRM2/+}$ mice,[14,29,30] C/EBPα-C^m alone induced AML with leukopenia in transplanted mice after BMT. We also confirmed the efficient induction of AML by coexpression of C/EBPα-C^m and C/EBPα-N^m. We will discuss the possible molecular mechanisms by which C/EBPα-N^m worked in concert with C/EBPα-C^m in accelerating leukemogenesis.

Methods

Patients and samples

We chose patients with hematologic diseases (224 MDS/AML patients, 71 therapy-related AML or MDS patients, and 89 de novo AML patients, who had been diagnosed at Hiroshima University Hospital between 1985 and 2007, are not a consecutive series of patients). All studies were approved by the Institutional Review Board at Hiroshima University and the ethics committee of the University of Tokyo (approval no. 20-10-0620). Patients' informed consents were obtained in accordance with the Declaration of Helsinki. *CEBPA* mutation screening by polymerase chain reaction (PCR)–single strand conformation polymorphism analysis and identification of *CEBPA*, *AML1*, *N-RAS*, *FLT3*, *PTPN11*, *C-KIT*, and *TP53* mutations was performed as described previously.[37]

Retroviral vectors

We used 2 C/EBPα mutants, N^m or C^m, as well as C/EBPα wild-type (WT) and C/EBPα N-terminal truncated p30 (p30). C/EBPα-WT, p30, N^m, or C^m, which was tagged with a FLAG or Myc epitope at the C terminus, was inserted upstream of the internal ribosome entry site-enhanced green fluorescent protein (IRES-EGFP) cassette of pMYs-IG to generate pMYs-FLAG or Myc-tagged CEBPα-WT, p30, N^m, or C^m-IG, respectively. Similarly, these fragments were subcloned into pMXs-IRES-puro (pMXs-IP), pMXs-IRES-blasticidin (pMXs-IB), or pMYs-IRES-dsRED (pMYs-IR). Flt3-ITD cDNA, which was derived from patient's leukemic cells harboring a 20-amino acid tandem duplication called M3[38,39] was subcloned into pMYs-IG to generate pMYs-Flt3-ITD-IG. Human granulocyte colony-stimulating factor receptor (G-CSF-R) cDNA, a kind gift from Dr Shigekazu Nagata (Kyoto University, Kyoto, Japan), was subconed into pMXs-IB to generate pMXs-G-CSF-R-IB.

Retroviral infection was done as described previously.[40] Briefly, retroviruses were generated by transient transfection of Plat-E packaging cells with FuGENE 6 (Roche Diagnostics).[41,42] Growth of transduced 32Dcl3 cells, which were subject to the drug selection with 1 μg/mL puromycin or 10 μg/mL blasticidin, was estimated by quantitating luminescence as described previously.[43]

Flow cytometric analysis

Briefly, cells were stained with phycoerythrin-conjugated antibodies (Abs) or biotinylated Abs and phycoerythrin/Cy5-streptavidin (eBioscience). Flow cytometric analysis of the stained cells was performed with FACSCalibur flow (BD Biosciences) equipped with FlowJo Version 7.2.4 software (TreeStar).

Real-time reverse-transcription PCR

Real-time reverse-transcription (RT) PCR was performed as described previously.[40] Reaction was subject to one cycle of 95°C for 30 seconds, 45 cycles of PCR at 95°C for 5 seconds, 55°C for 10 seconds, and 72°C for 10 seconds. The following primer pairs were used: 5′-AAGGCCCAGTGTGTCTCTGT-3′ (forward), and 5′-TACCAGCCCCAACTCAAAAC-3′ (reverse) for G-CSF-R, 5′-AGAGGGAAATCGTGCGTGAC-3′ (forward), and 5′-CAATAGTGATGACCTGGCCGT-3′ (reverse) for β-actin, 5′-GCCCCTAGTGCTGCATGAG-3′ (forward) and 5′-CCACAGACACCACATCAATTTCTT-3′ (reverse) for c-Myc.

Western blot analysis

Equal numbers of cells were lysed and Western blotting was performed as described previously.[35,40] Anti-Flag (M2) Ab (Sigma-Aldrich), anti-c-Myc (9E10) Ab (Roche Diagnostics), anti-C/EBPα (14AA) or (N-19) Ab (Santa Cruz Biotechnology), ERK1/2, signal transducer and activator of transcription (STAT)3, STAT5, AKT1, or Flt3 Abs, and phospho-STAT3 Ab (Santa Cruz Biotechnology), anti-phospho mitogen-activated protein kinase and phospho-AKT Abs (Cell Signaling Technology), and phospho-STAT5 Ab (BD Biosciences) were used.

Luciferase assay

The 293T cells were transiently transfected with the luciferase reporter plasmid p(C/EBP)2TK (kindly provided by Atsushi Iwama, Chiba University, Japan), pMXs-C/EBPα-WT or mutants-IP, and pEF-BOS/PU.1 for C/EBPα transcriptional activity, or E2Fx6-TATA-LUC, pCMV-E2F1, and pCMV-DP1 (kindly provided by Claus Nerlov, EMBL Mouse Biology Unit, Italy) for E2F transcriptional activity.[15] Luciferase assays were performed by Dual luciferase assay systems (Promega).

Immunostaining

Immunostaining of 293T cells transiently transfected with retrovirus constructs was performed as described previously.[35] After fixation with 1.5% paraformaldehyde, cells were immunostained with rabbit anti-Flag Ab or fluorescein isothiocyanate–conjugated mouse anti–c-Myc Ab (Sigma-Aldrich). The cells were then stained with Alexa Fluor 546–conjugated goat anti–rabbit immunoglobulin G secondary Ab (Molecular Probes). Nuclei were counterstained with Hoechst (H33342). Fluorescent images were analyzed on a confocal microscope (FLUOVIEW FV300 scanning laser biological microscope JX70 system; Olympus) equipped with SenSys/0L cold charge-coupled device (CCD) camera (Olympus). The objective lens (an LCPlanFI 60×/1.40 NA oil) was used.

Gel shift assay

Nuclear extracts from transfected 293T cells were incubated with 2 μg of polydeoxyinosinic-deoxycytidylic acid and then with double-stranded

Table 1. Clinical features and genetic findings of the patients with *CEBPA* mutations

Patient no.	Age, y/sex	Diagnosis	N terminal C terminal			Karyotype	Other gene mutation*	Survival (years)
			p30 type	bZIP inframe	Frameshift			
MDS/AML								
142	79/F	AML following MDS	I62fsX160	-	-	46,XY[20/20]	-	1.0
829	70/M	AML following MDS	P51fsX160	-	-	45,XY,der(17;18)(q10;q10)[2/20]/46,XY[18/20]	-	0.4
769	69/M	AML following MDS	-	R297P	-	46,XY[20/20]	*AML1, PTPN11*	1.6
896	77/M	AML following MDS	-	K313del	-	46,XY[20/20]	-	0.6
22	71/M	AML following MDS	-	-	G176fsX317	47,XY,+1,der(1;15)(q10;q10)[20/20]	-	0.8
679	89/M	MDS(RAEB)	-	-	P235fsX318	46,XY[20/20]	-	1.9
806	77/M	AML following MDS	G38fsX107	-	R291fsX313	46,XY[20/20]	-	1.9
Therapy-related AML or MDS								
59	80/F	AML(M4)	L19fsX159	-	-	47,XX,+8,t(9;11)(p22;q23)[20/20]	*AML1*	1.7
158	72/F	AML following MDS	F106fsX154	-	-	46,XX[20/20]	-	1.0
811	76/M	MDS(RAEB)	E59X†	-	-	46,XY[20/20]	-	1.7
1068	66/M	MDS(RAEB)	-	Q305P	-	46,XY[20/20]	-	> 1.5
346	59/M	AML following MDS	-	-	S190fsX320	43,XX,del(5)(q31),-7,-15,-18,-21,+mar [20/20]	*N-RAS*	0.8
577	56/F	AML following MDS	-	-	C213X	46,XX[20/20]	-	2.4
629	89/F	AML following MDS	-	-	L350fsX360	46,XX[20/20]	-	1.2
920	69/F	AML(M5)	-	-	S348fsX422	46,XX,t(11;17)(p15;q21)[20/20]	-	0.2
De novo AML(M2)								
40	68/F	AML(M2)	A111fsX166	S299_L304dup	-	46,XX[20/20]	-	> 10.5
292	75/F	AML(M2)	F33fsX107	R297P	-	46,XX[20/20]	-	> 8.4
662	58/F	AML(M2)	S65fsX167	K313dup	-	46,XX[20/20]	-	> 5.0
888	70/F	AML(M2)	A111fsX166	N321D	-	47,XX,+8[20/20]	-	> 3.8
941	31/F	AML(M2Eo)	T60fsX159	304_323dup	-	46,XX,del(7)(q32)[20/20]	-	> 3.5

RAEB indicates refractory anemia with excess blasts.
*Indicates that no mutation was detected in *AML1*, *N-RAS*, *FLT3*, *PTPN11*, *C-KIT*, and *TP53* genes.
†Homozygous mutation.

CSF3R promoter oligonucleotide labeled with γ^{32}P-adenosine triphosphate. Cold competition and a super-shift reaction were carried out by adding a 40-fold excess of cold CSF3R oligo or 1.5 μg of anti-C/EBP (14AA)X Ab (Santa Cruz Biotechnology), respectively. The resulting complexes were resolved on 4.5% polyacrylamide gel.[44]

Colony assay

Infected mouse bone marrow (BM) mononuclear cells (1×10^4) were plated in methylcellulose medium (StemCell Technologies) supplemented with 50 ng/mL each of interleukin (IL)–3, IL-6, stem cell factor, and granulocyte/macrophage-colony-stimulating factor (GM-CSF; R&D Systems) in the presence of 1 μg/mL puromycin. Colonies were counted after 1-week culture, and single-cell suspensions (10^4 cells) of drug-resistant colonies were subsequently replated.

Mouse BMT

Mouse BMT was performed as described previously.[40] Briefly, BM mononuclear cells were isolated from the femurs and tibias of C57BL/6 (Ly-5.1) donor mice 4 days after intraperitoneal administration of 150 mg/kg 5-fluorouracil. The cells were stimulated with 50 ng/mL of mouse stem cell factor, mouse FLT3 ligand, mouse IL-6, and human thrombopoietin (all cytokines were from R&D Systems). The prestimulated cells were infected for 60 hours with the retroviruses harboring pMYs-C/EBPα-C^m-IG, pMYs-C/EBPα-N^m-IG, pMYs-Myc-tagged C/EBPα-C^m-IG, pMYs-Flag-tagged C/EBPα-N^m-IR, pMYs-Flt3-ITD-IG, pMYs-IG, or pMYs-IR, using 6-well dishes coated with RetroNectin (Takara Bio). Then, $3\text{-}5 \times 10^5$ of the infected BM cells (that had not been sorted after either single or double infection) were injected into sublethally γ-irradiated C57BL/6 (Ly-5.2) recipient mice. Overall survival of transplanted mice were estimated using the Kaplan-Meier method. All animal studies were approved by the Animal Care Committee of the Institute of Medical Science, The University of Tokyo.

Statistical analysis

Statistical significance was calculated using the Student *t* test for independent variables. *P* values < .05 were considered statistically significant.

Results

CEBPA mutations in patients with myeloid malignancies

After we performed single-strand conformation polymorphism analysis to screen for *CEBPA* mutations in patients with hematologic disorders, *CEBPA* mutations were identified in 7 of 224 MDS/AML patients, 8 of 71 therapy-related AML or MDS patients, and 5 of 89 de novo AML patients (Table 1). Although the number of the de novo AML patients with *CEBPA* mutations were small, they all carried both an N-terminal mutation and a C-terminal bZIP in-frame mutation on the different alleles as reported previously.[20-26] On the other hand, most MDS/AML or therapy-related AML or MDS patients had single *CEBPA* mutations. As exceptions, we found both an N-terminal mutation and a

C-terminal frame-shift mutation in 1 case of AML after MDS (patient [Pt] #806) and homozygous N-terminal frame-shift mutations in one case of therapy-related MDS/RAEB (Pt #811). Examination of other genes (*RUNX1, N-RAS, FLT3, PTPN11, C-KIT,* and *TP53* gene) in these patients demonstrated that one case of MDS/AML (Pt #769) had both *RUNX1* and *PTPN11* mutations and that patients with therapy-related AML or MDS (Pt #59 or #346) had a mutation of *RUNX1* or of *N-RAS*, respectively. Consistent with recent reports,[22,26] our clinical data showed that overall survival was better in de novo AML patients with double *CEBPA* mutations compared with others with single *CEBPA* mutations (Table 1). These results suggested that double *CEBPA* mutations were able to induce AML, whereas single *CEBPA* mutation would lead to more aggressive AML, in concert with other gene alterations that have not been fully characterized.

The C-terminal but not N-terminal mutations of C/EBPα inhibited G-CSF–induced differentiation of 32Dcl3 cells into mature neutrophils

For further analysis, we chose an N-terminal mutant producing p30 designated as C/EBPα-N^m and a C-terminal b-ZIP in-frame mutant designated as C/EBPα-C^m (Figure 1A). C/EBPα-WT, C/EBPα-N^m, C/EBPα-C^m, C/EBPα-p30, or mock (pMXs-IP) was expressed in Plat-E cells. Expression of p42 protein or p30 protein generated by Myc-tagged C/EBPα-WT and mutants was verified by using anti-Myc Ab as bands corresponding to expected molecular weights (Figure 1B). In addition, we confirmed that N-terminal polypeptide produced by C/EBPα-N^m was detected by anti-C/EBPα Ab recognizing the N-terminal portion of C/EBPα (supplemental Figure 1, available on the *Blood* Web site; see the Supplemental Materials link at the top of the online article). Notably, the expression levels of p30 generated by C/EBPα-N^m were lower than those generated by C/EBPα-p30 (Figure 1B), indicating that deletion of the N-terminal part including the first start codon might increase the expression levels of p30 protein. We then infected 32Dcl3 cells with retroviruses harboring C/EBPα-WT or mutants, and the infected cells were subjected to drug selection. The 32Dcl3 cells expressing detectable levels of C/EBPα-WT were not obtained, presumably due to its strong inhibitory effect on proliferation. Western blot analysis showed that 32Dcl3 cells transduced with C/EBPα-C^m expressed the full length of C/EBPα-C^m at high levels (Figure 1B). C/EBPα-N^m or C/EBPα p30 transduced into 32Dcl3 cells was detected as a band (30 kDa), but the expression level of the former was much lower than that of the latter (Figure 1B). Growth speed was comparable among these transfectants in the presence of IL-3 (Figure 1C). However, the potential of these transfectants to differentiate in response to G-CSF varied; G-CSF treatment induced terminal differentiation of 32Dcl3 cells transduced with mock, as indicated by the appearance of polymorphonucleated neutrophils and up-regulation of CD11b on the surface (Figure 1D-E). G-CSF–induced granulocytic differentiation of 32Dcl3 cells was profoundly inhibited by C/EBPα-C^m, while it was only weakly inhibited by C/EBPα-N^m (Figure 1D-E). The differentiation was also attenuated by C/EBPα-p30, as reported previously.[45] We reasoned that the difference of 32Dcl3 cells expressing C/EBPα-N^m or C/EBPα-p30 in the granulocytic differentiation levels was due to the dissimilar expression levels of a short form of C/EBPα (30 kDa). As for the expression levels of G-CSF-R transcripts, a target of C/EBPα, they were extremely or moderately decreased in 32Dcl3 cells expressing C/EBPα-C^m or C/EBPα-p30, respectively, compared with other transfectants (Figure 1F), implicating G-CSF-R in induction of granulocytic differentiation. However, when human G-CSF-R was transduced into C/EBPα-C^m-expressing 32Dcl3 cells, G-CSF–induced granulocytic differentiation was not completely recovered (supplemental Figure 2). These results indicated that the differentiation block in 32Dcl3 cells expressing C/EBPα-C^m was presumably due to the suppression of C/EBPα activation, but not simply due to the decreased expression of G-CSF-R downstream of C/EBPα.[46]

C/EBPα-C^m or C/EBPα-N^m suppressed the transcriptional activity of C/EBPα-WT by different mechanisms

We next analyzed the transcriptional activation of C/EBPα-WT and mutants in 293T cells using a luciferase construct harboring 2 C/EBPα binding sites. As expected, C/EBPα-WT strongly activated this promoter, while neither C/EBPα-C^m, C/EBPα-N^m, nor C/EBPα-p30 showed any transcriptional activation (Figure 2A). We next examined whether these C/EBPα mutants affected the transcriptional activation of C/EBPα-WT. Although C/EBPα-C^m reduced G-CSF-R expression and inhibited G-CSF–induced myeloid differentiation of 32Dcl3 cells even more efficiently than C/EBPα-N^m (Figure 1D-F), C/EBPα-N^m as well as C/EBPα-p30 but not C/EBPα-C^m decreased promoter activity in the luciferase assay in 293T cells (top panel in Figure 2A), which was in accordance with the data shown by Gombart et al.[20] Expression of C/EBPα WT and mutants in the transfected 293T cells was verified by Western blot analysis (bottom panel in Figure 2A). These results indicated that C/EBPα-C^m and C/EBPα-p30 suppressed expression of G-CSF-R by different mechanisms. Interestingly, transcriptional activation of C/EBPα-WT drastically increased in 293T cells when coexpressed with PU.1, although PU.1 itself did not stimulate the same promoter (top panel in Figure 2B). Notably, this synergistic effect was suppressed by C/EBPα-C^m and weakly by C/EBPα-N^m with low expression levels of p30 protein (top panel in Figure 2B). Expression of C/EBPα and PU.1 was also confirmed by Western blot analysis (bottom panel in Figure 2B). Therefore, we assumed that C/EBPα-C^m was interacting with other transcription factors such as PU.1, thereby suppressing the activation of C/EBPα-WT in hematopoietic cells. We also tested whether the C/EBPα mutants inhibit E2F activity. However, neither C/EBPα-C^m nor C/EBPα-N^m repressed E2F1/DP1-mediated transcription (supplemental Figure 3). In this regard, there was no difference between C/EBPα-C^m and C/EBPα-N^m. We then compared the DNA-binding ability of C/EBPα-WT and mutants by electrophoresis mobility shift assay. As shown in Figure 2C, C/EBPα-WT protein bound to the CSF3R (G-CSF-R) probe, and C/EBPα-p30 protein generated by C/EBPα-N^m less efficiently bound to the same probe. Binding was verified by super-shift of the DNA-protein complex by the anti-C/EBPα Ab. Remarkably, C/EBPα-C^m failed to bind the CSF3R probe (Figure 2C). Next, we examined subcellular localization of C/EBPα-WT and mutants. In line with previous reports, C/EBPα-WT and mutants localized in the nucleus of the interphase cells (Figure 2D). However, it was noteworthy that unlike C/EBPα-WT and C/EBPα-p30, C/EBPα-C^m was not localized on chromosome during the mitotic phase (Figure 2D). It is possible that C/EBPα-C^m without a DNA binding ability is stealing some interacting protein from chromosome. Taken together, these results indicated that C/EBPα-N^m suppressed the transcriptional activation of C/EBPα-WT by its direct binding to the promoter or by its heterodimerization with C/EBPα-WT, while C/EBPα-C^m showed the suppressive effect indirectly, probably through interaction with other transcription factors such as PU.1.

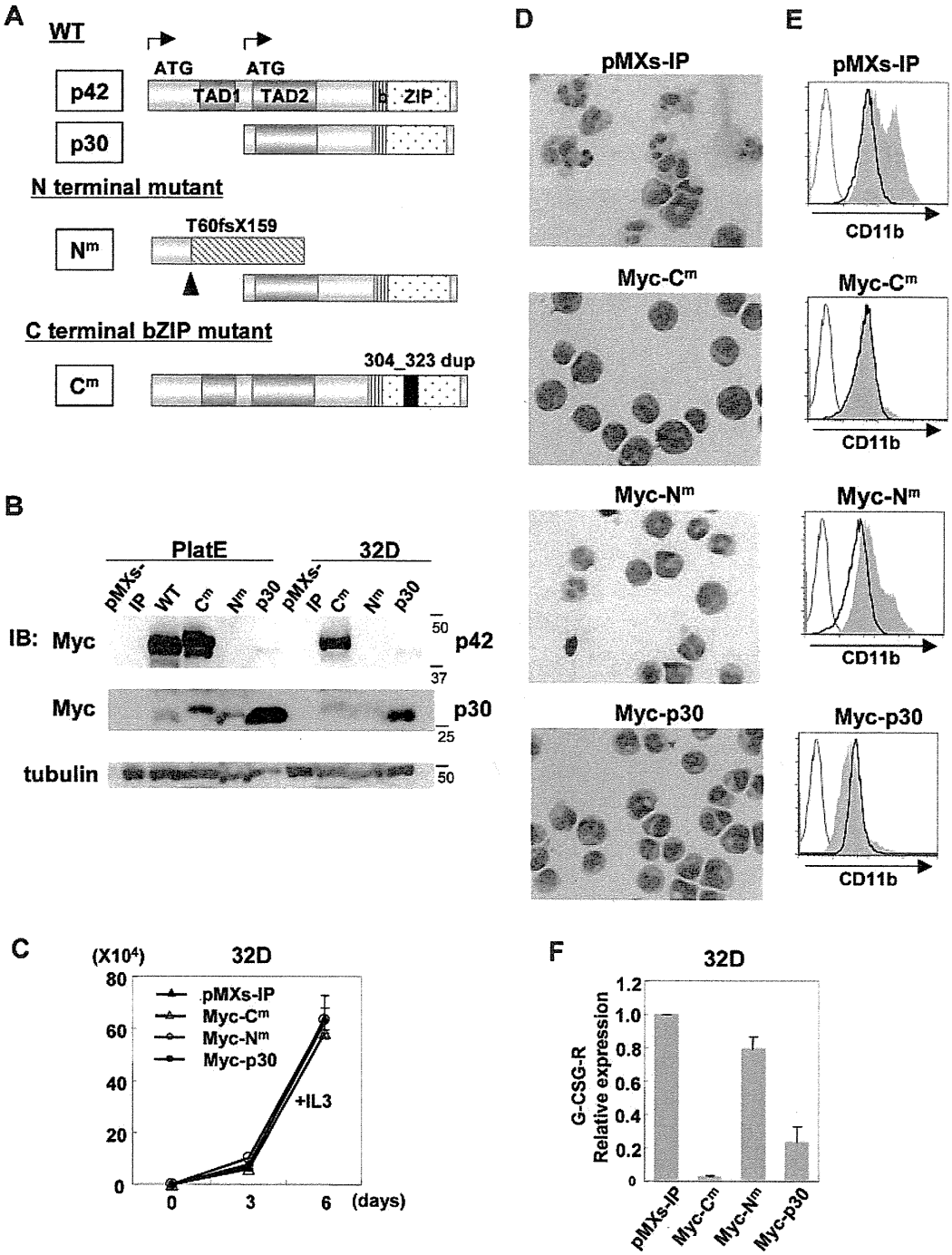

Figure 1. C/EBPα-C^m had the strong ability to block myeloid differentiation. (A) Schematic diagram of C/EBPα-WT (p42 and p30) and mutants, T60fsX159 (C/EBPα-N^m) and 304_323 dup (C/EBPα-C^m). TAD indicates the transcriptional activation domain; bZIP, basic region leucine zipper domain. (B) Expression of C/EBPα-WT and its mutants in Plat-E cells transiently transfected with a Myc-tagged C/EBPα-WT, C/EBPα-C^m, C/EBPα-N^m, or C/EBPα-p30 or an empty vector (pMXs-IP) and expression of C/EBPα mutants in 32Dcl3 cells transduced with Myc-tagged C/EBPα-C^m, C/EBPα-N^m, C/EBPα-p30, or mock (pMXs-IP). Cell lysates were subject to immunoblotting with anti-Myc Ab or anti-tubulin Ab as control. The results shown are representative of 3 independent experiments. (C) The growth of 32Dcl3 cells transduced with Myc-tagged C/EBPα-C^m, C/EBPα-N^m, C/EBPα-p30, or mock (pMXs-IP) in the presence of 1 ng/mL IL-3. All data points correspond to the mean and the standard deviation (SD) of 3 independent experiments. (D-E) 32Dcl3 cells transduced with Myc-tagged C/EBPα-C^m, C/EBPα-N^m, C/EBPα-p30, or mock (pMXs-IP) were cultured in the presence of 50 ng/mL G-CSF for 6 days. (D) Morphology of these cells was assessed by Giemsa staining. Images were obtained with a BX51 microscope and a DP12 camera (Olympus); objective lens, UplanFl (Olympus); original magnification ×40. (E) Surface expression of CD11b in these transfectants after incubation with 1 ng/mL IL-3 (bold histograms) or 50 ng/mL G-CSF (filled histograms) for 6 days was analyzed by flow cytometry. The result of control staining is shown as a thin-lined histogram. Data are representative of 3 independent experiments. (F) Relative expression levels of G-CSF-R in 32Dcl3 cells transduced with Myc-tagged C/EBPα-C^m, C/EBPα-N^m, C/EBPα-p30, or mock (pMXs-IP) were estimated by using real-time PCR. Data are representative of 3 independent experiments.

Retroviral transduction of C/EBPα-C^m, but not C/EBPα-N^m, immortalized BM hematopoietic cells

To determine the effect of C/EBPα-C^m and C/EBPα-N^m on differentiation and proliferation of hematopoietic cells, we performed serial colony-forming assays as described previously.[45] Mouse BM mononuclear cells were transduced with C/EBPα-C^m, C/EBPα-N^m, or C/EBPα-p30. Expression of C/EBPα mutants in the transduced BM cells was verified by Western blot analysis